Supporting Information

The Preparation of $CuInS_2$-ZnS-Glutathione Quantum Dots and its Application on the Sensitive Determination of Cytochrome c and Imaging of HeLa Cells

Xiangyang An[a], Yuemei Zhang[a], Jing Wang[a], De-ming Kong[a,b,c], Xi-wen He[a], Langxing Chen[*a,b,c], and Yukui Zhang[a,d]

[a]College of Chemistry, Nankai University, Tianjin 300071, P. R. China.

[b]Tianjin Key Laboratory of Biosensing and Molecular Recognition, Nankai University, Tianjin 300071, P. R. China.

[c]State Key Laboratory of Medicinal Chemical Biology, Nankai University, Tianjin 300071, P. R. China.

[d]Dalian Institute of Chemical Physics, Chinese Academy of Sciences, Dalian 116023, P. R. China.

Corresponding author: *Prof. L. X. Chen

E-mail: lxchen@nankai.edu.cn

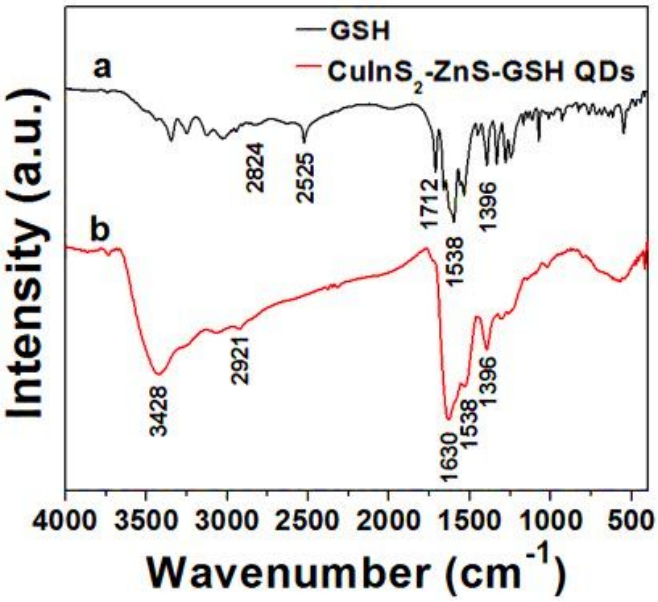

Figure S1. FT-IR spectrum of GSH (a) and $CuInS_2$-ZnS-GSH QDs (b).

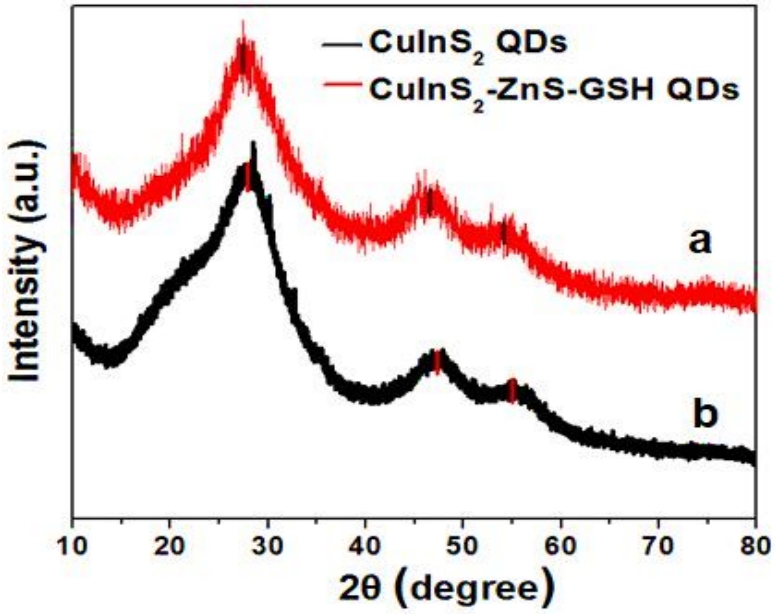

Figure S2. XRD patterns of $CuInS_2$-ZnS QDs (a) and $CuInS_2$-ZnS-GSH QDs (b).

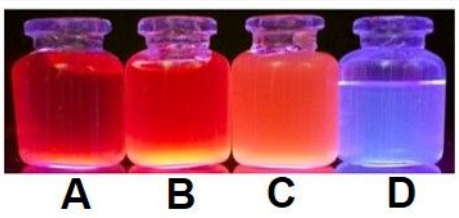

Figure S3. The influence of ZnS shell on the optical properties of $CuInS_2$ QDs. From left to right (A-D), the $CuInS_2$-ZnS-GSH QDs were prepared with molar mass of Cu^{2+} precursor of 0.01, 0.01, 0.01, and 0.0006 mmol, respectively, and the corresponding Zn^{2+} precursor of 0.16, 0.08, 0.01, and 0.01 mmol, respectively.

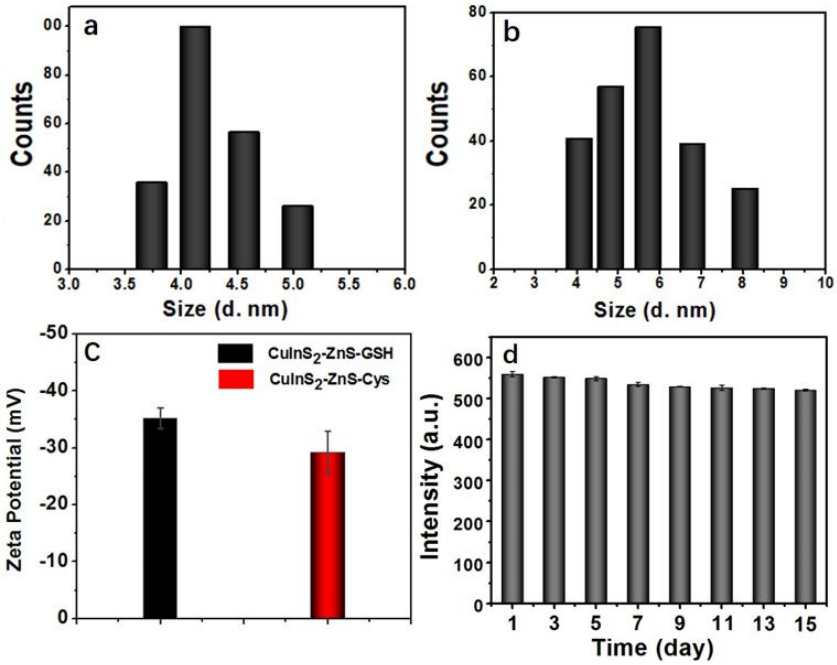

Figure S4. Hydrodynamic diameter variation of $CuInS_2$ (a) and $CuInS_2$-ZnS-GSH QDs (b). (c) The zeta potential of $CuInS_2$-ZnS-GSH QDs and $CuInS_2$-ZnS-Cys QDs in PBS (9.0). (d) PL intensity change of $CuInS_2$-ZnS-GSH QDs during a period of 15 days (n=3).

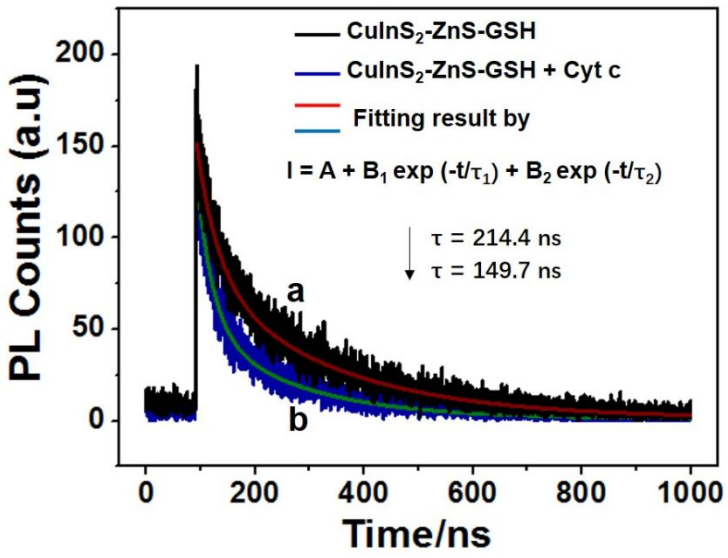

Figure S5. PL decay curve of $CuInS_2$-ZnS-GSH (a) and $CuInS_2$-ZnS-GSH QDs in Cyt c solution (b).

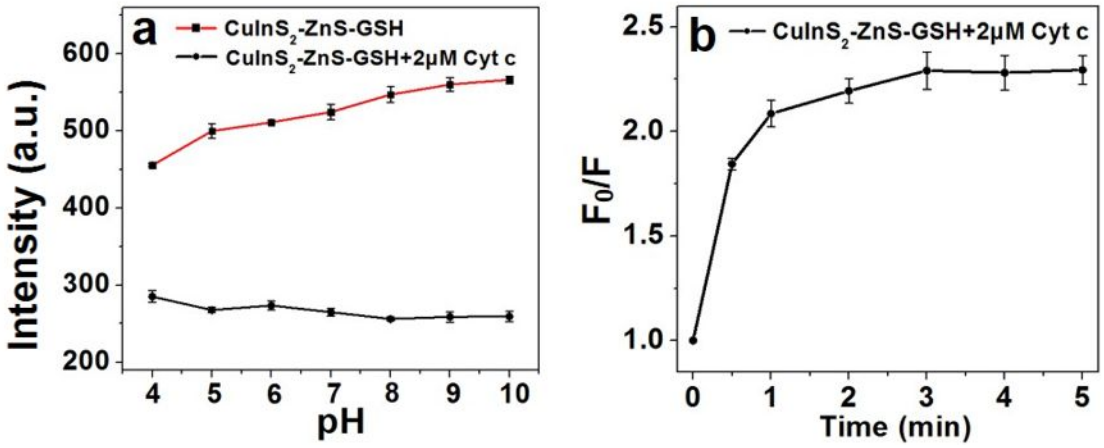

Figure S6. Effect of pH (a) and incubated time (b) on the detection of Cyt c by $CuInS_2$-ZnS-GSH QDs. The error bars represent the standard deviations from the mean of three independent experiments.

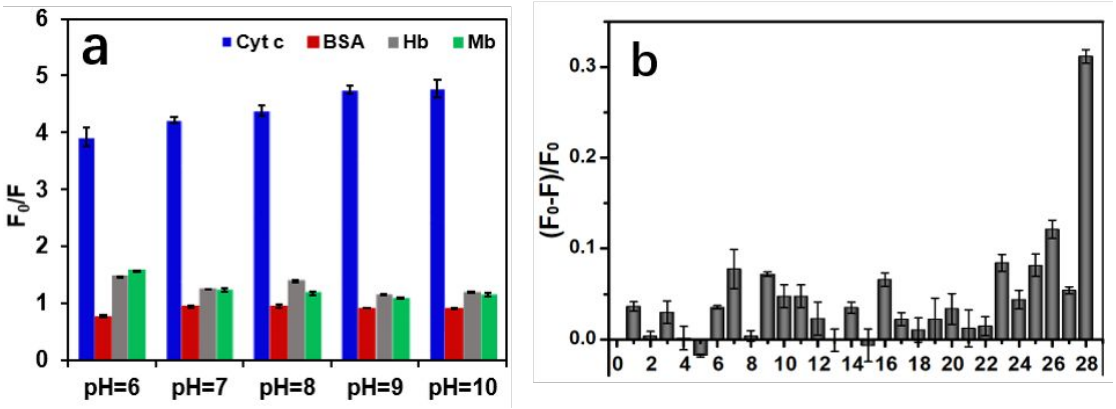

Figure S7. (a) The selectivity response of $CuInS_2$-ZnS-GSH QDs towards Cyt c, Mb, Hb and BSA at different pH in the presence of 10 μmol L^{-1} for Cyt c, BSA, Hb, and Mb respectively; (b) Selectivity of $CuInS_2$-ZnS-GSH QDs for Cyt c determination detection. From column 1 to 11, Cys, Glc, Asp, Tyr, Lys, Thr, Ser, Arg, Glu, ATP and urea at a concentration of 200 μmol L^{-1}; From column 12 to 21, Fe^{3+}, Na^{+}, K^{+}, Fe^{2+}, Ca^{2+}, Mg^{2+}, CO_3^{2-}, Cl^{-}, SO_4^{2-}, or NO_3^{-} at a concentration of 80 μmol L^{-1}; BSA, Hb, HSA, Mb, Lyz and IgG at a concentration of 2 μmol L^{-1}; Column 28, Cyt c at a concentration of 0.4 μmol L^{-1}. The error bars represent the standard deviations from the mean of three independent experiments.

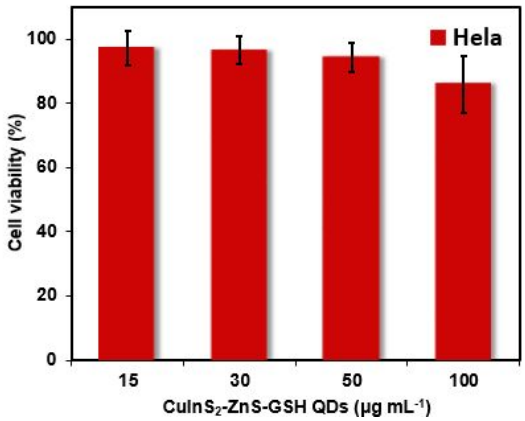

Figure S8. Cell viability of Hela cells in the presence of various concentration of $CuInS_2$-ZnS-GSH QDs. The error bars represent the standard deviations from the mean of three independent experiments.

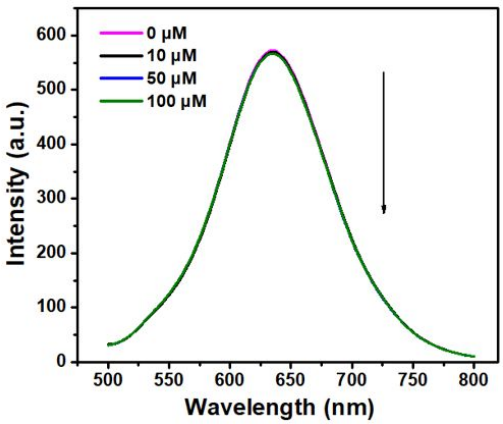

Figure S9. Fluorescence spectra of $CuInS_2$-ZnS-GSH QDs in the presence of various concentrations of etoposide.

Table S1. The PL lifetime of $CuInS_2$-ZnS-GSH QDs in PBS, Cyt c and BSA solution, respectively.

	χ^2	τ_1(ns)	Rel%	τ_2 (ns)	Rel%	τ (ns)
$CuInS_2$-ZnS-GSH	**1.109**	**38.8**	**12.77**	**240.1**	**87.23**	**214.4**
$CuInS_2$-ZnS-GSH +Cyt c	**1.078**	**29.1**	**21.10**	**182.0**	**78.90**	**149.7**
$CuInS_2$-ZnS-GSH QDs+BSA	**1.155**	**37.0**	**12.64**	**239.4**	**87.36**	**213.8**

Table S2. The comparison of methods for the determination of Cyt c.

Method	Material	Bioimaging	Detection range	Detection limit	Comment	Ref.
Turn-off fluorescence	Hb/Au NCs DNA/Ag NCs	embryonic kidney cells	0-10 μM 0-1.0 μM	14.3 nM 15.7 nM	Time,5 s; Aptamer,high-0cost; Relatively simple	1
HPLC		/	0-40 pM	0.1 pM	Time,20 min; Operation complex	2
Turn-on fluorescence	Aptamer/g-C_3N_4	Hela cells	16-140 nM	2.6 nM	Time,10 min; Aptamer,high-cost; low-toxicity	3
Fluorescence	GQDs/GO	A549 cells	0.25-14 μM	0.25 μM	Time,10 s; High detection limit ; low-toxicity	4
Turn-off fluorescence	TGA/CdTe QDs	SKIN cells	0.5-2.5 μM	0. 5 μM	narrow linearity range; heavy metal ion contained	5
Electrochemical	AuNP/PDA	/	0.1–100 μM	30 nM	Time 1 h, Antibody ,high cost; Operation complex	6
MIP	N-GQDs/SiO_2/MIP	/	0.2-60 μM	0.11 μM	Time 10 min; Operation complex	7
ICP-MS	Aptamer-AuNPs	/	0.1-20 nM	0.03 nM	Time 8 h; Instrument expensive; Aptamer,high cost	8
Turn-off fluorescence	CIS-ZnS-GSH QDs	Hela cells	0.01-7 μM	1.1 nM	Time 4 min; Laber-free, Low-cost; low- toxicity; high selectivity (Hb, Mb and BSA)	This work

References

1. Shamsipur, M., Molaabasi, F., Hosseinkhani, S. & Rahmati, F. Detection of Early Stage Apoptotic Cells Based on Label-Free Cytochrome c Assay Using Bioconjugated Metal Nanoclusters as Fluorescent Probes. *Anal. Chem.* **2016**, *88*, 2188-2197.

2. Crouser, E. D.; Gadd, M. E.; Julian, M. W.; Huff, J. E.; Broekemeier, K. M.; Robbins, K. A.; Pfeiffer, D. R. Quantitation of cytochrome c release from rat liver mitochondria. *Anal. Biochem.* **2003**, *317*, 67-75.

3. Salehnia, F.; Hosseini, M.; Ganjali, M. R. A fluorometric aptamer based assay for cytochrome C using fluorescent graphitic carbon nitride nanosheets. *Microchimica. Acta* **2017**, *184*, 2157-2163.

4. Cao, L.; Li, X. Q.; Qin, L. X.; Kang, S. Z.; Li, G. D. Graphene quantum dots supported by graphene oxide as a sensitive fluorescence nanosensor for cytochrome c detection and intracellular imaging. *J. Mater. Chem. B* **2017**, *5*, 6300-6306.

5. Amin, R. M.; Elfeky, S. A.; Verwanger, T.; Krammer, B. Fluorescence-based CdTe nanosensor for sensitive detection of cytochrome C. *Biosens. Bioelectron.* **2017**, *98*, 415-420.
6. Wen, Q.; Zhang, X.; Cai, J.; Yang, P. H. A novel strategy for real-time and in situ detection of cytochrome c and caspase-9 in Hela cells during apoptosis. *Analyst* **2014**, *139*, 2499-2506.
7. Yan, Y. J., He, X. W., Li, W. Y. & Zhang, Y. K. Nitrogen-doped graphene quantum dots-labeled epitope imprinted polymer with double templates via the metal chelation for specific recognition of cytochrome c. *Biosens. Bioelectron.* **2017**, *91*, 253-261.
8. Liu, J. M.; Yan, X. P. Ultrasensitive, selective and simultaneous detection of cytochrome c and insulin based on immunoassay and aptamer-based bioassay in combination with Au/Ag nanoparticle tagging and ICP-MS detection. *J. Anal. At. Spectrom.* **2011**, *26*, 1191-1197.